

FORMATION OF THE HOLOGRAPHIC SHEAR INTERFEROGRAMS BASED ON THE USE OF DIFFUSELY SCATTERED LIGHT FIELD FOR CONTROL OF THE TELESCOPE

V.G. Gusev

V.V. Kuibyshev State University, Tomsk

Received January 31, 1991

An analysis of a shear interferometer based on double-exposure recording of hologram of the image of a mat screen when the image is focused with a Kepler telescope is presented. It is shown both theoretically and experimentally that spatial filtration in the hologram plane enables one to control the field of the telescope. The spatial filtering in the Fourier plane makes it possible to record the interference pattern characterizing the phase distortions introduced in the wave illuminating the mat screen by the aberrations of the illuminating optical system.

In both classical and holographic shear interferometries based on recording the wavefronts we usually assume that all the optical parts of the interferometer are ideal and the errors due to them can be neglected in comparison with the errors due to the controllable objects. However, any actual interferogram is differential topography of the controllable object and incorporates the errors due to the interferometer itself. Because of this fact, the quality of the optical parts must meet stringent requirements and the interferograms themselves must be specially interpreted. For example, Refs. 1, 2, and 3 describe the technique for differential interferometry based on doubly exposed holograms of the focused image of a mat screen produced by a diffusely scattered radiation field. The diffusely scattered radiation fields make it possible to localize the interference patterns characterizing the controllable object and the optical parts used to form the reference beam and the illuminating wavefront in different planes. Therefore, the spatial filtration

enables one to record the shear interferogram characterizing solely the controllable object thereby resulting in the lenient requirements to the quality of the optical parts of the interferometer.

The well-known Kepler telescope is capable of forming the real image of the object. In the present paper we consider the formation of the shear interferograms based on doubly exposed holograms of the focused image of the mat screen produced by a diffusely scattered radiation field when the image is focused with the Kepler telescope.

As shown in Fig. 1 the image of the mat screen 1 is constructed in the plane of the photographic plate 2 with the telescope consisting of the positive lenses L_1 and L_2 . The hologram is produced during the first exposure by a quasiplanar reference wave 3. Prior to the second exposure the incidence angle of the quasiplanar illuminating wave is changed by α in the (x, z) plane while the incidence angle of the reference wave in the same plane is changed from θ_1 to θ_2 .

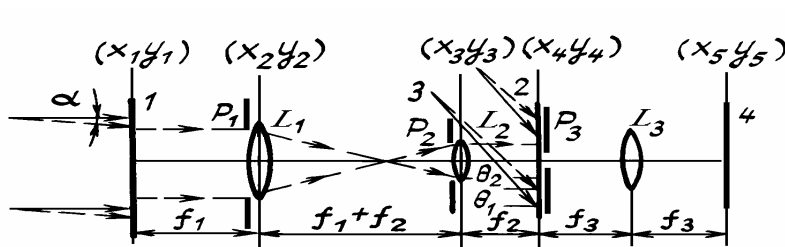


FIG. 1.

FIG. 1. Optical diagram of recording and reconstructing of the double exposure hologram of an image focused with the telescope: 1) mat screen; 2) photographic plate; 3) reference beam; 4) interferogram plane; L_1 , L_2 , and L_3 are lenses; p_1 and p_2 are aperture diaphragms and p_3 is a filtering diaphragm.

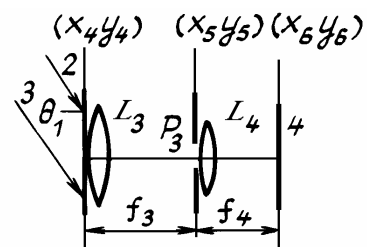


FIG. 2.

FIG. 2. Optical diagram of recording of the interference pattern localized in the hologram plane with spatial filtration in the Fourier plane.

Assuming that the diameter of the light beam incident on the mat screen exceeds the aperture diameter of the lens L_1 , we shall represent the complex amplitudes of the fields from the first and second

exposures in the (x_4, y_4) plane of the photographic plate in the Fresnel approximation, neglecting the amplitude and phase factors, which are constant in the plane:

$$\begin{aligned}
 u_1(x_4, y_4) \sim & \int \int \int \int \int \int_{-\infty}^{\infty} t(x_1, y_1) \exp i \varphi_1(x_1, y_1) \exp \left\{ \frac{ik}{2f_1} [(x_1 - x_2)^2 + (y_1 - y_2)^2] \right\} p_1(x_2, y_2) \times \\
 & \times \exp i \varphi_2(x_2, y_2) \exp \left[-\frac{ik}{2f_1} (x_2^2 + y_2^2) \right] \exp \left\{ \frac{ik}{2(f_1 + f_2)} [(x_2 - x_3)^2 + (y_2 - y_3)^2] \right\} p_2(x_3, y_3) \exp i \varphi_3(x_3, y_3) \times \\
 & \times \exp \left[-\frac{ik}{2f_2} (x_3^2 + y_3^2) \right] \exp \left\{ \frac{ik}{2f_2} [(x_3 - x_4)^2 + (y_3 - y_4)^2] \right\} dx_1 dy_1 dx_2 dy_2 dx_3 dy_3, \tag{1}
 \end{aligned}$$

$$\begin{aligned}
 u_2(x_4, y_4) \sim & \int \int \int \int \int \int_{-\infty}^{\infty} t(x_1, y_1) \exp i [kx_1 \sin \alpha + \varphi_1(x_1 + a, y_1)] \exp \left\{ \frac{ik}{2f_1} [(x_1 - x_2)^2 + (y_1 - y_2)^2] \right\} \times \\
 & \times p_1(x_2, y_2) \exp i \varphi_2(x_2, y_2) \exp \left[-\frac{ik}{2f_2} (x_2^2 + y_2^2) \right] \exp \left\{ \frac{ik}{2(f_1 + f_2)} [(x_2 - x_3)^2 + (y_2 - y_3)^2] \right\} \times \\
 & \times p_2(x_3, y_3) \exp i \varphi_3(x_3, y_3) \exp \left[\frac{ik}{2f_2} (x_3^2 + y_3^2) \right] \exp \left\{ \frac{ik}{2f_2} [(x_3 - x_4)^2 + (y_3 - y_4)^2] \right\} dx_1 dy_1 dx_2 dy_2 dx_3 dy_3, \tag{2}
 \end{aligned}$$

Here k is the wave number; $t(x_1, y_1)$ is the complex transmission amplitude of the mat screen and is a random function of the coordinates; $\varphi_1(x_1, y_1)$ is a deterministic phase function which characterizes the phase distortions of the illuminating wavefront due to aberrations in the illuminating optical system; $p_1(x_2, y_2) \exp i \varphi_2(x_2, y_2)$ is the generalized pupil function of the objective lens of the Kepler telescope (the lens L_1 with the focal length f_1 is shown in Fig. 1) and characterizes the axial wave

aberrations due to the objective lens; $p_2(x_3, y_3) \exp i \varphi_3(x_3, y_3)$ is the generalized pupil function of the eyepiece (the lens L_2 with the focal length f_2 is shown in Fig. 1); a is the illuminating wavefront shear resulting from the change in the wavefront tilt prior to the second exposure.

On the basis of expressions (1) and (2), the light fields in the back focal plane of the eyepiece may be represented by a convolution

$$\begin{aligned}
 u_1(x_4, y_4) \sim & \exp \left[\frac{ik}{2f_2} (x_4^2 + y_4^2) \right] \left\{ \left\{ \exp \left[-\frac{ik}{2f_2} (f_1 + f_2) (x_4^2 + y_4^2) \right] \right\} t(-\mu_1 x_4, -\mu_1 y_4) \times \right. \\
 & \left. \times \exp i \varphi_1(-\mu_1 x_4, -\mu_1 y_4) \left\{ \exp \left[-\frac{ik\mu_1^2}{2f_1} (x_4^2 + y_4^2) \right] \otimes P_1(x_4, y_4) \right\} \otimes P_2(x_4, y_4) \right\}; \tag{3}
 \end{aligned}$$

$$\begin{aligned}
 u_2(x_4, y_4) \sim & \exp \left[-\frac{ik}{2f_2} (x_4^2 + y_4^2) \right] \left\{ \left\{ \exp \left[\frac{ik}{2f_2} (f_1 + f_2) (x_4^2 + y_4^2) \right] \right\} t(-\mu_1 x_4, -\mu_1 y_4) \exp i \times \right. \\
 & \left. \times \left[-k \mu_1 x_4 \sin \alpha + \varphi_1(-\mu_1 x_4 + a, -\mu_1 y_4) + \frac{k\mu_1^2}{2f_1} (x_4^2 + y_4^2) \right] \otimes P_1(x_4, y_4) \right\} \otimes P_2(x_4, y_4) \Big\}, \tag{4}
 \end{aligned}$$

where \otimes denotes the convolution operation, $\mu_1 = \frac{f_1}{f_2}$ is the scale factor of image transformation,

$$\begin{aligned}
 P_1(x_4, y_4) &= \\
 &= \int \int_{-\infty}^{\infty} p_1(x_2, y_2) \exp i \varphi_2(x_2, y_2) \exp \left[-\frac{ik}{f_2} (x_2 x_4 + y_2 y_4) \right] dx_2 dy_2;
 \end{aligned}$$

$$\begin{aligned}
 P_2(x_4, y_4) &= \\
 &= \int \int_{-\infty}^{\infty} p_2(x_3, y_3) \exp i \varphi_3(x_3, y_3) \exp \left[-\frac{ik}{f_2} (x_3 x_4 + y_3 y_4) \right] dx_3 dy_3
 \end{aligned}$$

are the Fourier transforms of the generalized pupil functions of the objective lens and eyepiece, respectively.

As shown in Ref. 5, the width of the function $P_1(x_4, y_4)$ is of the order of $\frac{\lambda f_2}{d_1}$, where λ is the wavelength of the coherent light source used to record and reconstruct the hologram, d_1 is the diameter of the pupil of the objective lens. If the phase change of the spherical wave with radius of curvature $\frac{f_1}{\mu_1}$ does not exceed π within the domain of existence of the function $P_1(x_4, y_4)$, then this condition is satisfied in the (x_4, y_4) plane given that the diameter $D_1 \leq d_1 / \mu_1$. The term $\exp \left[\frac{ik\mu_1^2}{2f_1} (x_4^2 + y_4^2) \right]$ in expressions (3) and (4), which characterizes the phase distribution of a spherical wave can be taken outside the integral of convolution with the function $P_1(x_4, y_4)$, so that we obtain

$$u_1(x_4, y_4) \sim \exp\left[\frac{ik}{2f_2}(x_4^2 + y_4^2)\right] \left\{ \exp\left[-\frac{ik}{2f_2}(x_4^2 + y_4^2)\right] \times \right. \\ \left. \times \left[t(-\mu_1 x_4, -\mu_1 y_4) \exp i \varphi_1(-\mu_1 x_4, -\mu_1 y_4) \otimes P_1(x_4, y_4) \right] \otimes \right. \\ \left. \otimes P_2(x_4, y_4) \right\}, \quad (5)$$

$$u_2(x_4, y_4) \sim \exp\left[\frac{ik}{2f_2}(x_4^2 + y_4^2)\right] \left\{ \exp\left[-\frac{ik}{2f_2}(x_4^2 + y_4^2)\right] \times \right. \\ \left. \times \left[t(-\mu_1 x_4, -\mu_1 y_4) \exp i \left[-k\mu_1 x_4 \sin \alpha + \varphi_1(-\mu_1 x_4 + a, -\mu_1 y_4) \right] \otimes \right. \right. \\ \left. \left. \otimes P_1(x_4, y_4) \right] \otimes P_2(x_4, y_4) \right\}. \quad (6)$$

Since the width of the function $P_2(x_4, y_4)$ is of the order of $\frac{\lambda f_2}{d_2}$, where d_2 is the diameter of the pupil of the eyepiece, then within the domain of existence of the function $P_2(x_4, y_4)$ the phase change of the spherical wave with radius of curvature f_2 , given that the diameter $D_2 \leq d_2$, does not exceed π in the (x_4, y_4) plane. The term $\exp\left[-\frac{ik}{2f_2}(x_4^2 + y_4^2)\right]$ in expressions (5) and (6) can then be taken outside the integral of convolution with the function $P_2(x_4, y_4)$, and the distributions of the fields from the first and second exposures in the plane of the photographic plate given that $d_1 = \mu_1 d_2$ takes the form

$$u_1(x_4, y_4) \sim t(-\mu_1 x_4, -\mu_1 y_4) \exp i \varphi_1(-\mu_1 x_4, -\mu_1 y_4) \otimes \\ \otimes P_1(x_4, y_4) \otimes P_2(x_4, y_4), \quad (7)$$

$$u_2(x_4, y_4) \sim t(-\mu_1 x_4, -\mu_1 y_4) \exp i \left[-k\mu_1 x_4 \sin \alpha + \right. \\ \left. + \varphi_1(-\mu_1 x_4 + a, -\mu_1 y_4) \right] \otimes (P_1(x_4, y_4) \otimes P_2(x_4, y_4)). \quad (8)$$

Since both the objective lens and the eyepiece have finite dimensions and collect only a part of the spatial information which is carried by the light wave, it follows that each point of the object is broadened in the image plane to the speckle size which, in turn, is determined by the width of the function $P_1(x_4, y_4) \otimes P_2(x_4, y_4)$.

Let the double-exposure hologram recorded in this way be reproduced by a copy of the reference wave, e.g., from the first exposure. The diffraction field in the hologram plane is then given by

$$u(x_4, y_4) \sim t(-\mu_1 x_4, -\mu_1 y_4) \exp i \varphi_1(-\mu_1 x_4, -\mu_1 y_4) \otimes \\ \otimes P_1(x_4, y_4) \otimes P_2(x_4, y_4) + \exp i \left[kx_4(\sin \theta_1 - \sin \theta_2) + \right. \\ \left. \varphi_4(x_4, y_4) - \varphi_4(x_4 - b, y_4) \right] \left\{ t(-\mu_1 x_4, -\mu_1 y_4) \times \right. \\ \left. \exp i \left[-k\mu_1 x_4 \sin \alpha + \varphi_1(-\mu_1 x_4 + a, -\mu_1 y_4) \right] \otimes \right. \\ \left. \otimes P_1(x_4, y_4) \otimes P_2(x_4, y_4) \right\}, \quad (9)$$

where $\varphi_4(x_4, y_4)$ is the deterministic phase function characterizing the phase distortions introduced in the reference wavefront by the aberrations of the illuminating optical system, b is the reference wavefront shear caused by the change in the wavefront tilt prior to the second exposure.

If the condition $\sin \theta_1 - \sin \theta_2 = \mu_1 \sin \alpha$ is satisfied, then making use of the identity $\exp(ik\mu_1 x_4 \sin \alpha) \times \{t(-\mu_1 x_4, -\mu_1 y_4) \exp(-ik\mu_1 x_4 \sin \alpha) \otimes P_1(x_4, y_4) \otimes P_2(x_4, y_4)\} = t(-\mu_1 x_4, -\mu_1 y_4) \otimes \exp(ik\mu_1 x_4 \sin \alpha) [P_1(x_4, y_4) \otimes P_2(x_4, y_4)]$ which can be proved by representing the convolution in the integral form and by substituting the corresponding values of the Fourier transforms, we can write expression (9) in the form

$$u(x_4, y_4) \sim t(-\mu_1 x_4, -\mu_1 y_4) \exp i \varphi_1(-\mu_1 x_4, -\mu_1 y_4) \otimes \\ \otimes P_1(x_4, y_4) \otimes P_2(x_4, y_4) + \exp i \left[\varphi_4(x_4, y_4) - \right. \\ \left. - \varphi_4(x_4 - b, y_4) \right] \left\{ t(-\mu_1 x_4, -\mu_1 y_4) \exp i \varphi_1(-\mu_1 x_4 + a, -\mu_1 y_4) \otimes \right. \\ \left. \otimes \exp(ik\mu_1 x_4 \sin \alpha) \otimes [P_1(x_4, y_4) \otimes P_2(x_4, y_4)] \right\}. \quad (10)$$

From expression (10) it follows that in the hologram plane two identical speckle-fields from both exposures coincide with the speckle size determined by the width of the function $P_1(x_4, y_4) \otimes P_2(x_4, y_4)$. The whole speckle-field from the second exposure is tilted at the angle $\mu_1 \sin \alpha$ with respect to the optical axis. Hence it follows that the interference pattern, which characterizes the phase distortions of the illuminating wavefront and of the reference wavefront,¹ is localized in the hologram plane. Let the opaque screen p_3 with a circular aperture centered on the optical axis (Fig. 1) be positioned in the hologram plane. If the condition

$$\varphi_4(x_4, y_4) - \varphi_4(x_4 - b, y_4) - \varphi_1(-\mu_1 x_4, -\mu_1 y_4) + \\ + \varphi_1(-\mu_1 x_4 + a, -\mu_1 y_4) \leq \pi$$

is satisfied within the diameter of the aperture, i.e., if the diameter of the filtering aperture does not exceed the interference bandwidth of the interference pattern localized in the hologram plane, then the diffraction field at the exit from the filtering aperture is given by the expression

$$u(x_4, y_4) \sim p_3(x_4, y_4) \left\{ t(-\mu_1 x_4, -\mu_1 y_4) \otimes P_1(x_4, y_4) \otimes \right. \\ \left. \otimes P_2(x_4, y_4) + t(-\mu_1 x_4, -\mu_1 y_4) \otimes \exp(ik\mu_1 x_4 \sin \alpha) \times \right. \\ \left. \times [P_1(x_4, y_4) \otimes P_2(x_4, y_4)] \right\}, \quad (11)$$

where $p_3(x_4, y_4)$ is the transmission function of the opaque screen with a circular aperture.⁶

The light field in the recording plane 4 in Fig. 1 can be represented in the form of a Fourier integral of the field in the plane of spatial filtration. Then we obtain the following distribution of the correlating speckle-fields at the back focal plane of lens L_3 with focal length f_3

$$u(x_5, y_5) \sim \left\{ F \left[\frac{kx_5}{f_3}, \frac{ky_5}{f_3} \right] p_1(-\mu_2 x_5, -\mu_2 y_5) \times \right. \\ \left. \times p_2(-\mu_2 x_5, -\mu_2 y_5) \exp i \left[\varphi_2(-\mu_2 x_5, -\mu_2 y_5) + \right. \right.$$

$$\begin{aligned}
 & + \varphi_3(-\mu_2x_5, -\mu_2y_5)] + F \left[\frac{kx_5}{f_3}, \frac{ky_5}{f_3} \right] p p_1(-\mu_2x_5 + f_1 \sin \alpha, -\mu_2y_5) \times \\
 & \times p_2(-\mu_2x_5 + f_1 \sin \alpha, -\mu_2y_5) \exp i [\varphi_2(-\mu_2x_5 + f_1 \sin \alpha, -\mu_2y_5) + \\
 & + \varphi_3(-\mu_2x_5 + f_1 \sin \alpha, -\mu_2y_5)] \otimes P_3(x_5, y_5), \quad (12)
 \end{aligned}$$

where $\mu_2 = \frac{f_2}{f_3}$ is the scale factor of image transformation,

$$\begin{aligned}
 F \left[\frac{kx_5}{f_3}, \frac{ky_5}{f_3} \right] p &= \int_{-\infty}^{\infty} \int_{-\infty}^{\infty} t(-\mu_1x_4, -\mu_1y_4) \times \\
 & \times \exp \left[-\frac{ik}{f_3}(x_4x_5 + y_4y_5) \right] dx_4 dy_4;
 \end{aligned}$$

$$P_3(x_5, y_5) = \int_{-\infty}^{\infty} \int_{-\infty}^{\infty} p_3(x_4, y_4) \exp \left[-\frac{ik}{f_3}(x_4x_5 + y_4y_5) \right] dx_4 dy_4;$$

are the Fourier transforms of the corresponding functions.

From expression (12) it follows that in the Fourier plane the identical speckles coincide within the region of overlap of the images of the exit pupil of the Kepler telescope. Hence it follows that the interference pattern is localized in the focal plane of the lens L_2 . Indeed, if the period of oscillation of the function $\exp i [\varphi_2(-\mu_2x_5, -\mu_2y_5) + [\varphi_3(-\mu_2x_5, -\mu_2y_5) + \exp i [\varphi_2(-\mu_2x_5 + f_1 \sin \alpha, -\mu_2y_5) + \varphi_3(-\mu_2x_5 + f_1 \sin \alpha, -\mu_2y_5)]]$ exceeds the speckle size determined by the width of the function $P_3(x_5, y_5)$ in the (x_5, y_5) plane by an order of magnitude,⁷ this function can be taken outside the convolution integral in expression (12). The superposition of the correlating speckle-fields then results in the irradiance distribution of the form

$$\begin{aligned}
 I(x_5, y_5) &\sim \{1 + \cos[\varphi_2(-\mu_2x_5, -\mu_2y_5) + \varphi_3(-\mu_2x_5, -\mu_2y_5) - \\
 &- \varphi_2(-\mu_2x_5 + f_1 \sin \alpha, -\mu_2y_5) - \varphi_3(-\mu_2x_5 + f_1 \sin \alpha, -\mu_2y_5)] \otimes
 \end{aligned}$$

$$\begin{aligned}
 & u(x_5, y_5) \sim \exp \left[\frac{ik}{2f_3}(x_5^2 + y_5^2) \right] \left\{ F_1 \left[\frac{kx_5}{f_3}, \frac{ky_5}{f_3} \right] p_1(-\mu_2x_5, -\mu_2y_5) p_2(-\mu_2x_5, -\mu_2y_5) \exp i [\varphi_2(-\mu_2x_5, \right. \\
 & -\mu_2y_5) + \varphi_3(-\mu_2x_5, -\mu_2y_5) + \Phi(x_5, y_5) \otimes F_2 \left[\frac{kx_5}{f_3}, \frac{ky_5}{f_3} \right] p_1(-\mu_2x_5 + f_1 \sin \alpha, -\mu_2y_5) \times \\
 & \left. \times p_2(-\mu_2x_5 + f_1 \sin \alpha, -\mu_2y_5) \exp i [\varphi_2(-\mu_2x_5 + f_1 \sin \alpha, -\mu_2y_5) + \varphi_3(-\mu_2x_5 + f_1 \sin \alpha, -\mu_2y_5)] \right\}, \quad (14)
 \end{aligned}$$

where

$$\begin{aligned}
 F_1 \left[\frac{kx_5}{f_3}, \frac{ky_5}{f_3} \right] &= \int_{-\infty}^{\infty} \int_{-\infty}^{\infty} t(-\mu_1x_4, -\mu_1y_4) \exp i \varphi_1(-\mu_1x_4, -\mu_1y_4) \exp \left[-\frac{ik}{f_3}(x_4x_5 + y_4y_5) \right] x_4 dy_4; \\
 F_2 \left[\frac{kx_5}{f_3}, \frac{ky_5}{f_3} \right] &= \int_{-\infty}^{\infty} \int_{-\infty}^{\infty} t(-\mu_1x_4, -\mu_1y_4) \exp i \varphi_1(-\mu_1x_4 + a, -\mu_1y_4) \exp \left[-\frac{ik}{f_3}(x_4x_5 + y_4y_5) \right] dx_4 dy_4; \\
 \Phi(x_4, y_4) &= \int_{-\infty}^{\infty} \int_{-\infty}^{\infty} \exp i [\varphi_4(x_4, y_4) - \varphi_4(x_4 - b, y_4)] \exp \left[-\frac{ik}{f_3}(x_4x_5 + y_4y_5) \right] dx_4 dy_4.
 \end{aligned}$$

are the Fourier transforms of the corresponding functions.

$$\otimes \left| F \left[\frac{kx_5}{f_3}, \frac{ky_5}{f_3} \right] \otimes P_3(x_5, y_5) \right|^2, \quad (13)$$

which describes the speckle-structure modulated by the interference fringes. The interference pattern has the form of shear interferogram in the fringes of infinite width, which characterizes the axial wave aberrations due to the Kepler telescope.

According to expression (11), the information on the phase distortions introduced in the wavefront of the light wave by the aberrations of the objective lens and the eyepiece is embedded within the individual speckle in the hologram plane. Now the distribution of the field within each individual speckle is determined by the convolution $P_1(x_4, y_4) \otimes P_2(x_4, y_4)$ within the small element of the image of the mat screen on the optical axis and is formed as a result of diffraction of the wave with zero spatial frequency of the hologram of the mat screen by the pupils of the objective lens and the eyepiece of this telescope. The interference pattern characterizing the axial wave aberrations of the telescope is recorded with the spatial filtration following the above-described optical scheme. As to the small element of the image of the mat screen centered at the off-axis point with coordinates $(x_{40}, 0)$, the amplitude-phase distribution of the field within an individual speckle in this region is the result of

diffraction of the wave with the spatial frequency $\frac{x_{40} \mu_1}{\lambda f_2}$

by the mat screen. Hence it follows that the off-axis spatial filtration results in forming the interference pattern which in a combined way characterizes the on-axis and off-axis wave aberrations due to the Kepler telescope.

To record the interference pattern localized in the hologram plane, we consider the spatial filtration of the light field reconstructed from a double-exposed hologram in the Fourier plane (Fig. 2).

If we assume that the diameter of the lens L_3 positioned in the hologram plane is greater than the size of the image of the mat screen, we may write the expression for the diffraction field in the back focal plane of the lens L_3 on the basis of expression (10):

If the condition $\varphi_2(-\mu_2x_5, -\mu_2y_5) + \varphi_3(-\mu_2x_5, -\mu_2y_5) - \varphi_2(-\mu_2x_5 + f_1\sin\alpha, -\mu_2y_5) - \varphi_3(\mu_2x_5 + f_1\sin\alpha, -\mu_2y_5) < \pi$ is satisfied within the diameter of the aperture diaphragm p_3 of the lens L_4 (Fig. 2) centered on the optical axis, i.e., if the diameter of the filtering aperture does not exceed the width of the interference pattern localized in the Fourier plane, then the diffraction field at the exit from the aperture is given by the expression:

$$u(x_5, y_5) \sim p_3(x_5, y_5) \exp\left[\frac{ik}{2f_3}(x_5^2 + y_5^2)\right] \left\{ F_1 \left[\frac{kx_5}{f_3}, \frac{ky_5}{f_3} \right] + \Phi(x_5, y_5) \otimes F_2 \left[\frac{kx_5}{f_3}, \frac{ky_5}{f_3} \right] \right\}. \quad (15)$$

The diffraction field in the back focal plane of the lens L_4 (Fig. 2) with the focal length f_4 can be represented as a Fourier integral of the field in the plane of spatial filtration multiplied by the phase distribution of the spherical wave. The distribution of the correlating speckle fields in the recording plane 4 (Fig. 2) then is given the form:

$$u(x_6, y_6) \sim \exp\left[\frac{ik}{2f_4}(x_6^2 + y_6^2)\right] \left\{ \left\{ t(\mu_1\mu_3x_6, \mu_1\mu_3y_6) \exp i\varphi_1 \times \right. \right. \\ \left. \left. \times (\mu_1\mu_3x_6, \mu_1\mu_3y_6) + t(\mu_1\mu_3x_6, \mu_1\mu_3y_6) \exp i[\varphi_4(-\mu_3x_6, -\mu_3y_6) - \right. \right. \\ \left. \left. - \varphi_4(-\mu_3x_6 - b, -\mu_3y_6) + \varphi_1(\mu_1\mu_3x_6 + a, \mu_1\mu_3y_6)] \right\} \otimes P_4(x_6, y_6) \right\} \quad (16)$$

where $\mu_3 = f_3/f_4$ is a scale factor of image transformation, and

$$P_4(x_6, y_6) = \int_{-\infty}^{\infty} \int_{-\infty}^{\infty} p_3(x_5, y_5) \exp\left[\frac{ik}{2f_3}(x_5^2 + y_5^2)\right] \times \\ \times \exp\left[-\frac{ik}{f_4}(x_5x_6 + y_5y_6)\right] dx_5 dy_5$$

is the Fourier transform of the corresponding function.

As follows from expression (16), the identical speckles in the (x_6, y_6) plane coincide within the region of overlap of the images of the mat screen. If the period of oscillations of the function $\exp i\varphi_1(\mu_1\mu_3x_6, \mu_1\mu_3y_6) + \exp i[\varphi_4(-\mu_3x_6, -\mu_3y_6) - \varphi_4(-\mu_3x_6 - b, -\mu_3y_6) + \varphi_1(\mu_1\mu_3x_6 + a, \mu_1\mu_3y_6)]$ exceeds the speckle size determined by the width of the function $P_4(x_6, y_6)$, then this function can be taken outside the convolution integral in expression (16). In this case the irradiance distribution is formed by the superposition of the correlating speckle-fields

$$I(x_6, y_6) \sim \left\{ 1 + \cos[\varphi_4(-\mu_3x_6, -) - \varphi_4(-\mu_3x_6, -b, -\mu_3y_6) + \varphi_1(\mu_1\mu_3x_6 + a, \mu_1\mu_3y_6) - \varphi_1(\mu_1\mu_3x_6, \mu_1\mu_3y_6)] \times \right. \\ \left. \times \left| t(\mu_1\mu_3x_6, \mu_1\mu_3y_6) \right\} \otimes P_4(x_6, y_6) \right|^2 \quad (17)$$

which describes the speckle structure modulated by the interference fringes. The interference pattern then has the form of a shear interferogram in fringes of infinite width

which characterizes the phase distortions introduced in the reference and illuminating wavefronts by the aberrations of the illuminating optical systems.

In our experiment we recorded the double-exposure holograms of the image of the mat screen when the image is focused with the Kepler telescope on Micrat-VRL photographic plates using a He-Ne laser with wavelength $\lambda = 0.63 \mu\text{m}$. A VU - 200 autocollimator served as a controlled telescope. The image of the screen in the plane of the photographic plate was constructed with this telescope at 21X magnification. Prior to the second exposure, the angle α of the wavefront tilt of the wave incident on the mat screen was equal to $57'47''$ while $\Delta\theta = 2'45''$ to an accuracy of $\pm 3''$. The double-exposure hologram was reproduced by a small-aperture laser beam of $\approx 2 \text{ mm}$ in diameter, and the interference pattern was recorded in the focal plane of the objective lens of 8 cm in focal length. Figure 3a shows an interferogram filtered with the help of reconstruction of the hologram at the on-axis point. This interference pattern characterizes a spherical aberration with post-focal defocusing at the pupil of the telescope 5 mm in diameter. The interference pattern filtered with the help of reconstruction of the hologram at a point with coordinates $x_{40} = 8 \text{ mm}$ and $y_{40} = 0$ is shown in Fig. 3b.

According to Ref. 8 taking into account the defocusing T , the relation for the third-order aberrations as functions of coordinates (x, y) of the exit pupil of the telescope takes the form

$$\varphi(x, y) = A(x^2 + y^2)^2 + B(x_4x + y_4y)(x^2 + y^2) + \\ + C(x_4^2 + y_4^2)(x^2 + y^2) + D[(x_4^2 - y_4^2)(x^2 - y^2) + 4x_4y_4xy] + \\ + E(x_4^2 + y_4^2)(x_4x + y_4y) + T(x^2 + y^2),$$

where A, B, C, D , and E are the coefficients characterizing the spherical aberration, the coma, the curvature of the field, the astigmatism, and the distortion, respectively. In Fig. 3a the interferogram can be interpreted using the method proposed in Ref. 9, which is based on the assumption that the functions determining both the unknown wavefront and the fringes in the shear interference pattern are "smooth" and may be related to each other. This yields $A = 24$ and $T = 12.1$ in units of the wavelength. Using these data, the interferogram from Fig. 3b was interpreted, and the coefficients characterizing the deformation in a plane wave propagating at an angle $\beta = 2^\circ 18'$ with respect to the optical axis, when the deformation was produced by the off-axis aberrations, were determined as follows: $B = 7.1$ and $(C + D) = 4.3$.

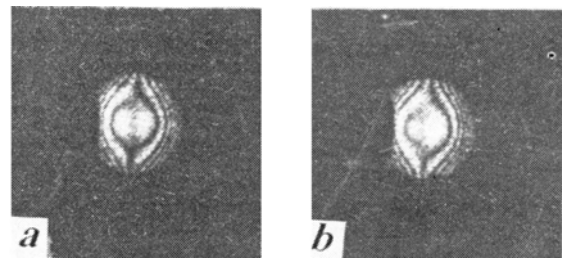


FIG. 3. Shear interferograms localized in the Fourier plane and recorded when performing the spatial filtration on-axis (a) and off-axis (b).

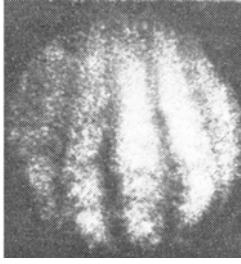


FIG. 4. Shear interferogram localized in the hologram plane.

Figure 4 shows the interference pattern localized in the hologram plane. To record it in accordance with Fig. 2 the lens 25 cm in focal length and the objective lens 8 cm in focal length were used. The spatial filtration was performed in the Fourier plane on the optical axis. The diameter of a filtering aperture was about 1.5 mm. Since the Kepler telescope has no the vignetting effect,¹⁰ and the speckles in the hologram plane are oriented along the optical axis,¹¹ the interference picture localized in the hologram plane can be recorded in this way when the hologram is reconstructed in the plus-first order of diffraction. In addition, in both cases the telescope can be used, which forms an image in the hologram plane, with spatial filtration in the Fourier plane.

To summarize the results of our theoretical analysis and the experimental data, it should be noted that the considered technique of differential interferometry with the help of the diffusely scattered fields based on double-exposure records of the holograms of the image of the mat screen, when the image is focused with a Kepler telescope,

results in the shear interference pattern localized in the hologram plane and in the far-diffraction zone. Spatial filtering in the hologram plane makes it possible to record the shear interferograms independently within the region of overlap of the images of the exit pupil of the telescope. This shear interferogram characterizes the wave aberrations due to the telescope. Phase distortions of the illuminating and reference wavefronts due to aberrations in the illuminating optical systems do not result in any change of the filtered interference patterns.

REFERENCES

1. V.G. Gusev, *Atm. Opt.* 3, No. 9, 857–866 (1990).
2. V.G. Gusev, *Atm. Opt.* 3, No. 10, 947–956(1990).
3. V.G. Gusev, *Atm. Opt.* 4, No. 3, 211–217(1990).
4. J. Goodman, *Introduction to Fourier Optics*. (McGraw–Hill, New York, 1968).
5. M. Franson, *Optics of the Speckles* [Russian translation] (Mir, Moscow, 1980), 158 pp.
6. M. Born and E. Wolf, *Principles of Optics*, 4th ed. (Pergamon Press, Oxford, 1970).
7. R. Jones and K. Wikes, *Holographic and Speckle–Interferometry* [Russian translation] (Mir, Moscow, 1986), 320 pp.
8. M. Menu and I. Roblin, *J. Optics (Paris)* 10, No. 1, 1–11 (1979).
9. D. Dutton, A. Cornejo, and M. Latta, *Appl. Optics* 7, No. 1, 125–131 (1968).
10. M.I. Apenko and A.S. Dubovik, *Applied Optics* (Nauka, Moscow, 1982), 348 pp.
11. I.S. Klimenko, *Holography of Focused Images and Speckle–Interferometry* (Nauka, Moscow, 1985), 217 pp.